11-10-2017

Comparing Laser Diffraction and Optical Microscopy for Characterizing Superabsorbent Polymer Particle Morphology, Size, and Swelling Capacity

Cole R. Davis

Stacey L. Kelly

Kendra Erk

Comparing Laser Diffraction and Optical Microscopy for Characterizing Superabsorbent Polymer Particle Morphology, Size, and Swelling Capacity

Cole R. Davis · Stacey L. Kelly · Kendra A. Erk*

School of Materials Engineering, Purdue University, 701 West Stadium Avenue, West Lafayette, IN 47907 USA

*corresponding author: erk@purdue.edu, 1-765-494-4118

Abstract

This study determined the accuracy and practicality of using optical microscopy (OM) and laser diffraction (LD) to characterize hydrogel particle morphology, size, and swelling capacity. Inverse suspension polymerized polyacrylamide particles were utilized as a model system. OM and LD showed that the average particle diameter varied with mixing speed during synthesis for dry (10-120 μm) and hydrated (34-240 μm) particles. LD volume and number mean diameters showed that few, large particles were responsible for the majority of water absorption. Excess water present in gravimetric swelling measurements led to larger swelling capacities (8.2 ± 0.37 g/g) while volumetric measurements using OM and LD resulted in reduced capacities (6.5 ± 3.8 g/g and 5.7 ± 3.9 g/g respectively). Results from individual particle swelling measurements using OM (5.2 ± 0.66 g/g) statistically confirmed that the volumetric methods resulted in a reduced and more accurate measurement of swelling capacity than the gravimetric method.

1 Introduction

Superabsorbent polymer (SAP) hydrogels are crosslinked polymer networks, capable of absorbing and releasing large amounts of water. These chemical crosslinks prevent the SAP from being dissolved in water during the absorption process [1–5]. With this absorption capability, hydrogels have been found useful in concrete curing [6–10], biomedical applications [11–13], oil recovery [14,15] and much more. Of the many SAPs available for use, polyacrylamide (PAM) and PAM-based hydrogels are broadly researched due to their low cost and ease of preparation [2,11]. SAP hydrogels are typically prepared via bulk polymerization [5,8,13], emulsion polymerization [13,14] or inverse suspension polymerization [2,16,17]. Of these, inverse suspension polymerization is often preferred

over other methods due to better heat dissipation during polymerization, lower viscosity of the reaction mixture [2], formation of spherical particles and control of the particle size by altering variables like mixing speed, crosslinking agent and surfactant [3,16].

Before use, SAP particles must be characterized in order to control and achieve a desired morphology, particle size distribution (PSD), and swelling behavior.

Characterization of particle morphology is required to determine the correct methods for size and swelling capacity characterization, which will be discussed later. Not only is morphology a critical factor in deciding which method to use, but particle size and swelling capacity are also important factors to consider when these particles are used in various applications. For example, in concrete applications, SAP morphology will determine the shape and size of the pores that remain in the concrete microstructure, potentially reducing the strength of the cured concrete [18,7,9]. Directly linked to particle size is perhaps the most important property of SAPs – their swelling capacity. This will not only determine how large the particles swell when immersed in fluid but also how much solvent the SAP can retain and ultimately release into the concrete to aid in curing and prevent volumetric shrinkage and cracking of the concrete[18,19]. Workability of concrete is also affected by the addition of SAPs and is governed by swelling capacity [10,19]. Characterization of these properties are also important in biomedical applications [13,20]. In drug delivery, for example, the swelling capacity affects how much of a drug can be transported by the SAP particles [12,21].

Many different methods have been used to characterize SAP particles. For example, morphology is commonly investigated using scanning electron microscopy (SEM) for dry particles [16], environmental SEM (ESEM) for hydrated particles [17], transmission electron microscopy (TEM) [22] and optical microscopy (OM) [14].

PSDs have been characterized using sieves, microscopy, the Coulter principle, dynamic light scattering (DLS) and laser diffraction (LD). Using sieves to determine a PSD results in a discontinuous size distribution with large fractional size ranges [8,23]. While microscopy techniques are accurate and are often used to determine particle sizes [14,22,24,25], they require image processing which can be time consuming, and the sample size is limited to the number of particles within a micrograph and the number of micrographs taken. To reduce the time required and increase the sample size, particle size analyzers can be used to obtain accurate PSDs. One method employs the

Coulter principle but has been shown to underestimate particle sizes of hydrogels in the swollen state [25]. DLS and LD are preferred methods due to their relatively fast analysis time and accuracy. DLS, however, can only be used for particles up to several microns [2,22,26] whereas LD can measure particle sizes ranging from 0.04 μm to 2,000 μm. Particle size measurements over this range make LD a common method for determining the size distribution of micrometer-sized SAPs [16,20,21,24,26,27].

One limitation of LD is the requirement for the particles being measured to be spherical, and it cannot be used to accurately measure the size distribution of irregularly shaped (non-spherical) particles. LD uses optical models that calculate the diameters of particles from scattered light measurements. These diameters are then used to create a size distribution based off of the volume fraction to which each particle belongs [28]. Irregularly shaped particles have larger average diameters than a spherical particle of an equivalent volume and results in an overestimation of particle size when measuring irregularly shaped particles [23]. Measurements using this method are often reported as an average volume mean diameter (d_{V-LD}) but can also be reported as surface area mean (d_{SA-LD}) and number mean (d_{N-LD}) diameters. Volume mean diameter describes the particles that make up the majority of the sample's volume; surface area mean diameter is used to determine what size particles make up the majority of the sample's specific surface area; and number mean diameter describes how many particles are present at a given size [29].

SAP swelling behavior has been studied using many techniques, including the gravimetric method and variations of this. The gravimetric (tea bag) method uses a filter bag to submerge a known amount of dry SAP into a solution to determine how much of this solution the SAP can absorb. Periodic mass measurements are made until equilibrium (maximum absorbency) is reached at which point the swelling ratio, or swelling capacity, (Q) is calculated. When the filter bag containing SAP is removed from the solution, it is suspended, allowing any excess solution to drip off [3,8]. This method of removing excess water can lead to an overestimation of the swelling capacity due to the excess solution that may be contained between particles and within the filter bag [3,28]. Variations of the gravimetric method aim at eliminating this source of error by using centrifugal techniques [27], vacuum filtering [30] and blotting with filter paper [1,4,13,17,31]. Even with these improved techniques, gravimetric swelling measurements are less accurate when compared to volumetric swelling measurements [2].

Measurements of swelling capacity through the volumetric method involve particle size analysis in the dry and hydrated states. This is performed with spherical particles so that a change in diameter from the dry to hydrated state can be directly related to a change in volume. A change in volume upon addition of a wetting solution can be contributed to the absorption of the solution. Using the densities of the SAP and the solution being absorbed, the mass of dry SAP and the mass of absorbed solution can be calculated, respectively. These masses can then be used to determine Q. Using a change in volume from size measurements eliminates the chance of including surface water to the swelling capacity of the SAP, making this method more accurate than the methods previously described [28]. It has been shown that the swelling capacity of SAP hydrogels can be studied using DLS [2], OM [24] and LD [20,21,26–28].

This study used inverse suspension polymerized PAM to compare OM and LD particle size and swelling capacity measurements in search for faster and more accurate characterization methods. Volume, surface area, and number mean diameter LD PSDs were investigated along with OM PSDs. Hydrogel swelling behavior was determined and compared using the gravimetric method and the volumetric method through OM and LD.

2 Materials and Methods

2.1 Materials and Synthesis

PAM was custom synthesized from acrylamide (AM) (Sigma Aldrich) through inverse suspension polymerization. Cyclohexane (225 mL) and Span-80 (0.75 g) constituted the continuous phase. Prepared separately, the aqueous phase proportions are located in Table 1. Reverse osmosis (RO) water, AM and N,N'-methylenebisacrylamide (MBAM) were mixed together until AM was dissolved, approximately 20 minutes. Sodium persulfate (NaPS) was then mixed in for 30 seconds. Aqueous and continuous phases were mixed together in a round bottom flask, using an overhead mixer, for 2 hours under a continuous nitrogen purge. Controlled mixing speeds of 400, 500, 600, 800, 1000 and 1200 rpm were used to create different particle sizes. Polymerization was initiated upon addition of tetramethylethylenediamine (TMED) and heating to 65 °C. Mixing continued for 5 hours, until polymerization was complete. Synthesized SAP particles were rinsed with RO water, ethanol, and acetone and dried at room temperature for 48 hours.

Table 1: Proportions of each component in the aqueous phase for synthesis of PAM particles.

Hydrogel	AM (g)	RO Water (ml)	MBAM (g)	NaPS (ml)	TMED (ml)
PAM	2.4	12	0.05	1	1.3

2.2 Morphology and Size Characterization

OM was used to characterize the morphology of dry and hydrated SAP particles. Two methods were used to determine the average diameter and size distribution for each sample: OM paired with ImageJ and LD. OM analysis was used by taking three to five micrographs of dry and hydrated SAP particles. Dry SAP particles were not suspended in any liquid and were air dried for at least 24 hours. A thin layer of dry SAP particles were spread onto a glass slide. Hydrated particles were suspended in nanopure water (Barnstead Nanopure Infinity D50250), and a pipette was used to transfer the hydrated particles onto a glass slide with excess water to prevent the particles from drying. From these micrographs, between 50 and 300 (depending on particle size and magnification) particles were selected randomly and their diameters (d_{OM}) were measured using ImageJ. These measurements are reported as a number mean diameter with an error of one standard deviation.

Size characterization using LD (Beckman Coulter LS230) was used for dry and hydrated particles to obtain d_{V-LD}, d_{SA-LD}, and d_{N-LD} size distributions. Between 0.10 and 0.20 grams of dry and hydrated SAP particles were suspended in 20.0 mL of 2-propanol and nanopure water, respectively. All samples were then sonicated for one hour to eliminate particle agglomeration. LD works by casting a light source onto suspended particles and correlating the light scattered by the particles to their size. To determine this correlation, computer software uses the refractive index of the particle and solvent along with the Mie scattering model to generate a volume mean diameter size distribution which can then be converted to number and surface area mean diameter size distributions [28,29].

2.3 Swelling Tests

Swelling capacity was characterized using the gravimetric method. Nylon filter bags with a pore size of 5 microns (supplied by The Cary Company; catalog number: 21WNWF) were used to

submerge a pre-weighed amount of dry SAP into nanopure water. These bags were weighed at time intervals of 0.5, 1, 3, 5, 10, 15, 30 and 60 minutes to determine their gravimetric swelling capacity (Q_g) over time. Each swelling test was performed three times. The swelling capacity was calculated by using the mass of the wet bag (m_{bag}), mass of the dry SAP (m_{dry}) and mass of the SAP and bag after submersion (m_{wet}) along with Equation 1.

$$Q_g = \frac{m_{wet} - m_{dry} - m_{bag}}{m_{dry}} \quad \textbf{(1)}$$

Swelling capacity was also determined using the volumetric method. Dry and hydrated diameters were collected during size characterization using OM and LD. These diameters were converted to particle volume and the change in volume from the dry state (V_d) to the hydrated state (V_h) was contributed to the absorption of water. This change in volume along with the density of water (ρ_{H20}=1.00 g/cm^3) gave the mass of water absorbed by the SAP. Mass of the SAP was calculated by using the dry volume and the density of the SAP being used (ρ_{SAP}). Density of PAM was assumed to be 1.30 g/cm^3 [33]. Using this along with Equation 2, the volumetric swelling capacity (Q_V) was calculated. All swelling measurements are reported with 95% confidence intervals.

$$Q_V = \frac{(V_h - V_d) * \rho_{H20}}{V_d * \rho_{SAP}} \quad \textbf{(2)}$$

3 Results and Discussion

3.1 Morphology

Micrographs of dry and hydrated (in nanopure water for 24 hours) particles are shown in Figure 1. Both samples were synthesized at a mixing speed of 500 rpm. Figure 1A shows that inverse suspension polymerization leads to micrometer-sized spherical particles. These particles appear uniform in their shape but vary in diameter. Some dry particles contain voids on their surface which are most likely caused by inconsistencies in crosslinking density during synthesis. Areas of low crosslinking density may act as pores causing the surface of the polymer to collapse when dried, resulting in a surface defect. Figure 1B shows that when hydrated, the SAP hydrogels

remain spherical in shape as their diameters increase. Under visual inspection alone, it is clear that the hydrated particles increase in size and become more transparent, indicating water absorption.

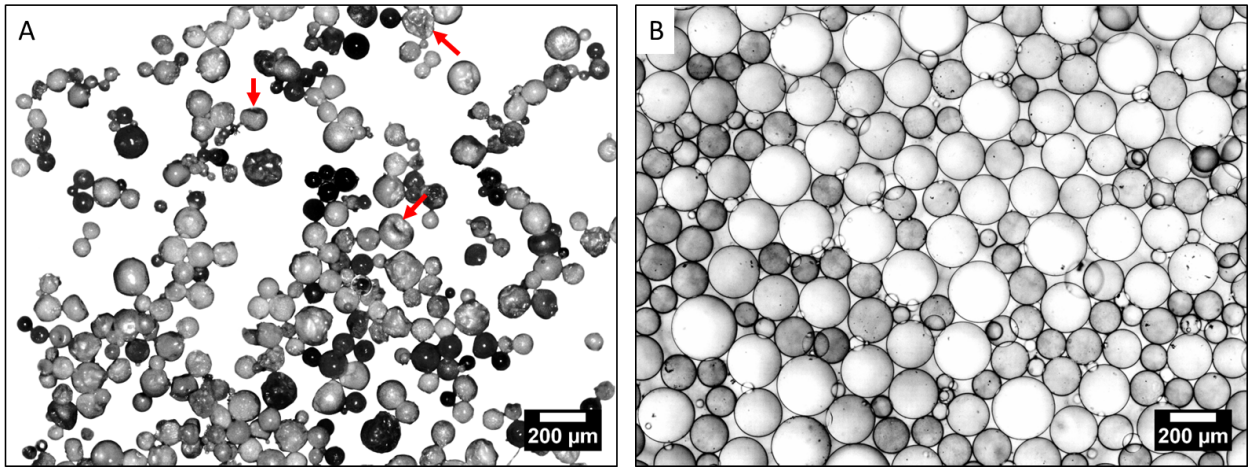

Figure 1: Micrograph of dry PAM (A) and PAM hydrated in nanopure water (B) synthesized at 500 rpm. Red arrows in micrograph A point out surface voids on dry particles. Scale bars are 200 µm.

It is not always the case that these hydrated particles are spherical. It was found that when preparing a hydrated sample for LD particle size measurements, if stirring was performed with a stir bar, then the hydrated spheres would break apart, as seen in Figure 2. Fracture of spheres during mixing did not occur for dry particles in 2-propanol. This indicates that the mechanical strength of the particles is reduced when they are hydrated and should be considered when choosing an application for SAP particles of this type. Fracturing of particles during mixing occurred consistently with all samples of PAM and because of this, sonication is preferred to suspend particles in a solvent or non-solvent. No fracture was found at stir times less than 1 hour or during sonication.

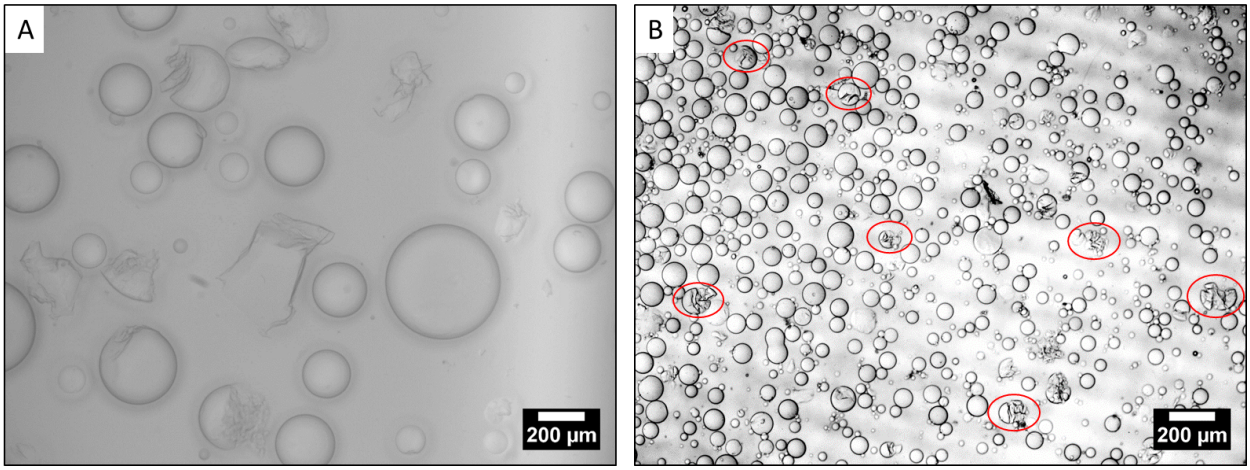

Figure 2: Micrographs of hydrated PAM particles synthesized at 400 rpm (A) and 1000 rpm (B). These hydrated sample were stirred with a stir bar for 2 hours causing the particles to break apart (indicated in image B by the red ovals). Scale bars are 200 µm.

3.2 Optical Microscopy Size Analysis

Average dry and hydrated particle diameters for PAM using OM paired with ImageJ are shown in Figure 3. Dry (un-hydrated) average particle diameters range from 10 to 120 µm and hydrated diameters range from 34 to 240 µm depending on the mixing speed. As the mixing speed increases, the average particle diameter decreases for both dry and hydrated PAM. This is expected because as the mixing speed increases, there is more turbulence in the suspension mixture, making it more likely for the droplets to break up into smaller sizes [34]. The reverse of this is also expected because if the suspension mixture is stirred very slowly or not stirred at all, then the two phases will separate due to immiscibility and density mismatch and the polymerized product will be a single macroscale object, similar to bulk polymerization [35]. It can also be seen that as mixing speed increases, the standard deviation of particle size decreases for dry and hydrated PAM as well. This suggests that at high mixing speeds, the particle sizes are more uniform and the sample has a narrow PSD relative to lower mixing speeds.

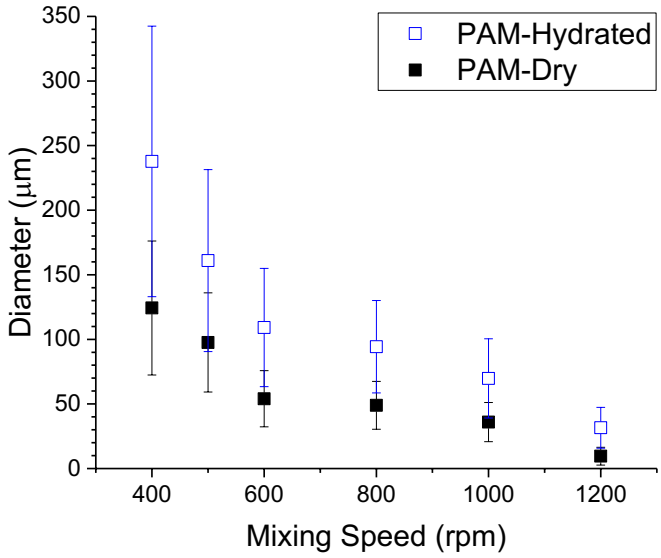

Figure 3: Dry (solid black squares) and hydrated (open blue squares) number mean diameters of PAM particles using optical microscopy. Error bars represent one standard deviation.

Hydrated size distributions for particles synthesized at mixing speeds of 400 rpm and 1000 rpm can be found in Figure 4A and Figure 4B respectively along with micrographs of each sample. Both distributions were made from 200 particle measurements using OM paired with ImageJ. This illustrates that as the mixing speed increases, the average particle size and the size distribution decrease.

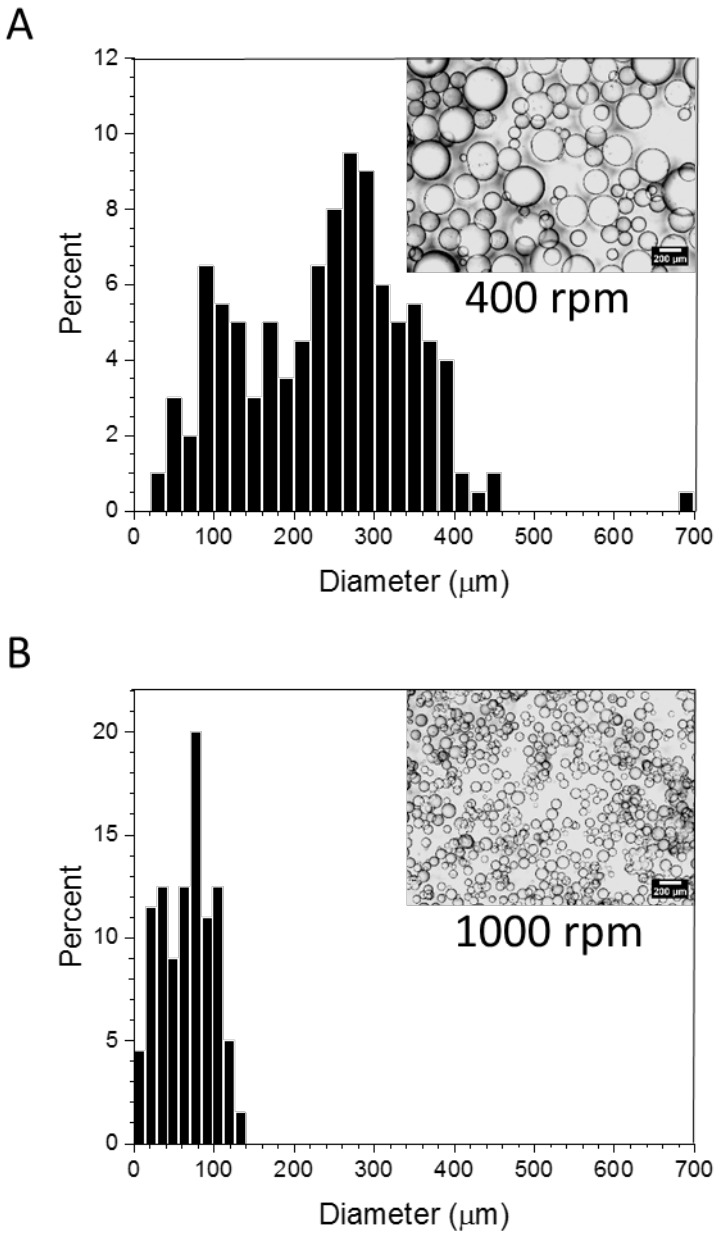

Figure 4: Number mean diameter particle size distributions for hydrated PAM at mixing speeds of 400 rpm (A) and 1000 rpm (B). Both size distributions were created from 200 particle measurements using OM paired with ImageJ. Micrographs of each sample are located in the upper right corner of each plot for visual size comparison. Scale bars are 200 μm.

3.3 Laser Diffraction Particle Size

Several solvents were tested to suspend dry PAM particles for use in the LD analyzer, including ethanol, 2-propanol, pyridine, cyclohexane, and hexanes. Table 2 presents all of the solvents tested, their effects on swelling and clumping of SAPs, and their dielectric constants. A

solvent was needed that would prevent the dry particles from clumping and also not be absorbed by the hydrogel. Clumping is undesirable because several small agglomerated particles will appear as one large particle and the size of this larger agglomerate is not an accurate representation of the individual particle sizes. Likewise, if any absorption occurs then the size of the particle will change due to swelling and the SAP will no longer be considered dry.

Table 2: Dielectric constants at 20 °C for LD suspension solvents and their effects on clumping and swelling of PAM.

Solvent	**Clump**	**Swell**	**ε** [32]
Water	No	Yes	80.1
Ethanol	No	No	25.3
2-propanol	No	No	20.2
Pyridine	Yes	No	13.3
Cyclohexane	Yes	No	2.02
Hexanes	Yes	No	1.89

Hydrogen bonding is partially responsible for the absorption of solvents within the hydrogel due to the particles' amide groups [4,36]. Therefore, for accurate LD measurements of un-hydrated particle size, hydrogen bonding capabilities of the solvent must be weak or not present in order to prevent swelling as well as particle aggregation. Ethanol and 2-propanol successfully prevented the PAM particles from aggregating as well as swelling [37]. To demonstrate this, micrographs were taken of individual dry particles in the presence and absence of solvent. Figure 5 shows that the addition of ethanol and 2-propanol do not seem to significantly impact the volume of the SAP particle under the timescales of observation (approximately 30 minutes).

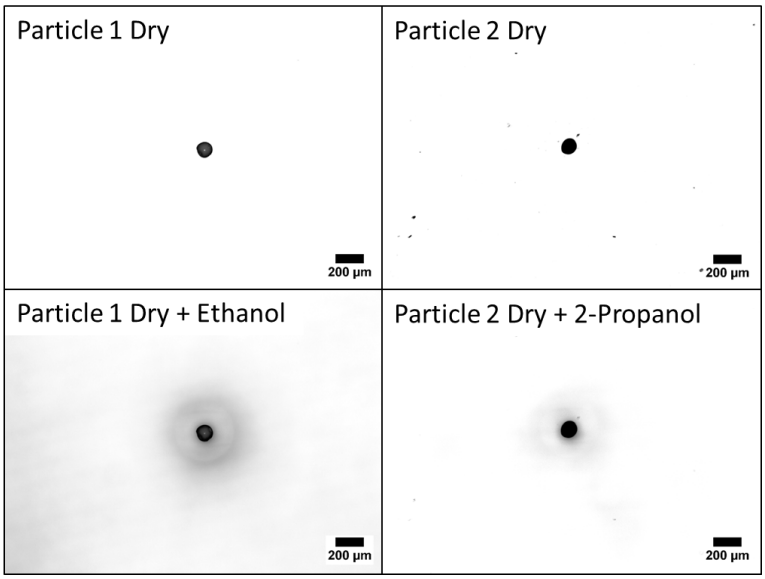

Figure 5: Micrographs of individual dry PAM particles mixed at 500 rpm without and with the addition of ethanol (left) and 2-propanol (right).

Upon further investigation using ImageJ, it was found that the particles in solvent did have a slight increase in diameter on the order of several microns (5 µm increase for ethanol and 6 µm increase for 2-propanol). This increase in size could be due to a layer of solvent creating a dome on top of the particle resulting in a lensing effect. Evidence of this lensing effect can be seen by the halo of distorted light around each particle in the images containing solvent. However, if this is not a lensing effect and the particles do increase by several microns, it is negligible considering the particles being measured are over 100 µm in diameter (112 µm for particle 1 and 110 µm for particle 2). If we assume that the particles do not swell in ethanol or 2-propanol and they are swelling slightly, the error associated with diameter measurements using LD will be less than 6%.

Pyridine, cyclohexane, and hexanes were not capable of swelling PAM due to their inability to hydrogen bond. However, the particles were observed to aggregate within these non-polar solvents, most likely due to the polar chemical structure of PAM which promoted particle aggregation in order to reduce particle-solvent interaction. A solvent with a relatively large dielectric constant is more polar than a solvent with a lower dielectric constant [38,39]. Using this information, a solvent can be selected that is polar enough to minimize particle aggregation but not so polar as to induce swelling. Isopropanol (2-propanol) was selected for measurement using

LD due to the value of its dielectric constant relative to the solvents previously mentioned and successfully prevented aggregation while not swelling PAM.

PSDs from the LD analyzer can be reported in three ways; number, surface area, and volume mean diameters. Figure 6A and Figure 6B show all three size distributions for PAM synthesized at 400 rpm and 1000 rpm respectively. Number mean diameter contains information on how many particles, out of the total number of particles, are in a specific size range. All particle sizes are evenly weighted in these distributions. Surface area mean diameter can be used to determine what size particles are responsible for the majority of water transfer at the water-particle interface. These size distributions are more weighted towards large particles than number diameter and can be seen by a size distribution shift toward the right. Volume mean diameter can be used to determine what size particles are responsible for the majority of swelling and water storage in the hydrated state. These size distributions are the most heavily weighted towards large particles, resulting in a large shift to the right in the PSD curve. All three size distributions contain valuable information that can be used to describe the particle system.

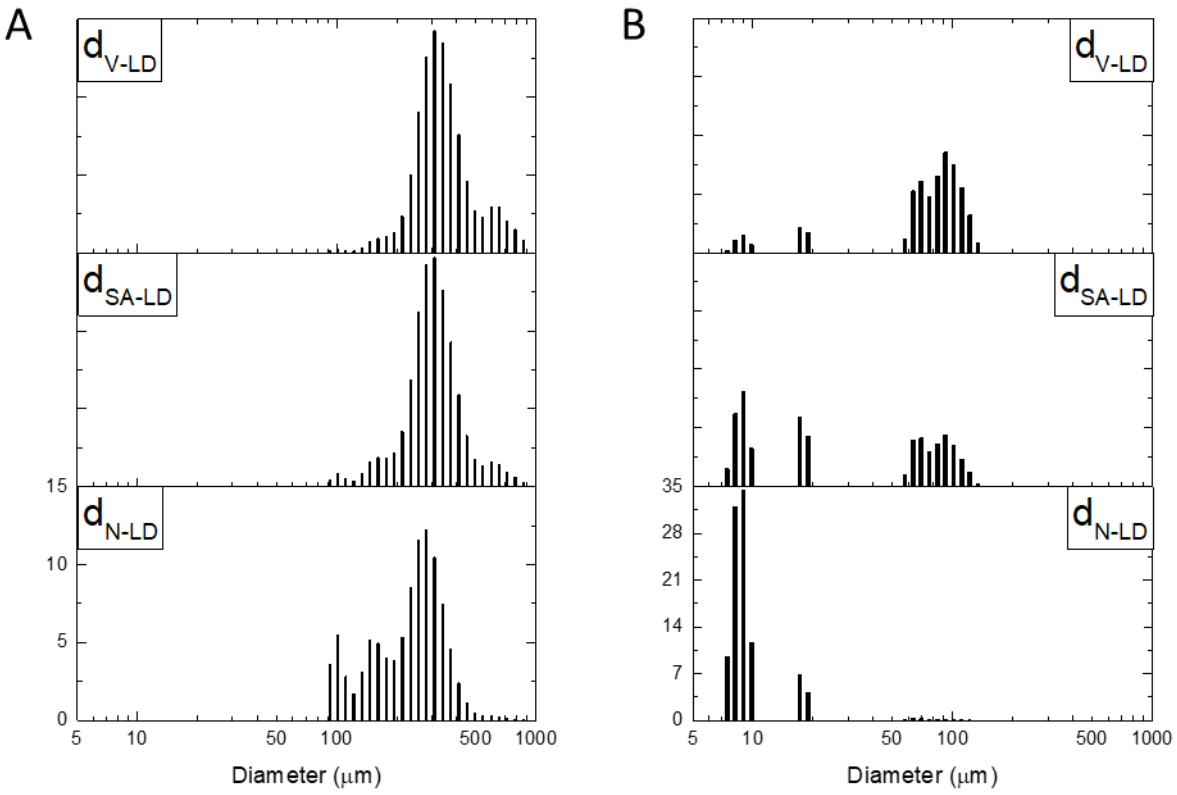

Figure 6: LD size distributions for hydrated PAM at mixing speeds of 400 rpm (A) and 1000 rpm (B) in number, surface area and volume mean diameter.

Comparing Figure 6 with Figure 4 shows that LD is capable of identifying large and small particles more readily than OM. For example, a single particle (0.5% of all particles measured) over 500 μm was identified using OM while more particles (1.1% of all particles) were identified between 500 and 1000 μm when using LD. Large particles are less likely to be observed and measured through OM because there are fewer of these particles. Even though there are relatively few, large particles are important to identify because they are responsible for the majority of the swelling and water storage. Figure 6B (d_{N-LD}) shows that the majority of the particles are between 8 and 10 μm whereas Figure 4B (d_{OM}) suggests that the majority of the particles are between 20 and 100 μm. The lack of small particles being measured when using OM could be due to the visual obstruction of small particles by larger ones, making small particles less likely to be observed and measured. Also, depending on the magnification being used, small particles could be out of focus

and cannot be measured as easily as larger particles. LD has greater measurement sensitivity due to constant mixing of the sample and by measuring a larger sample size.

Average dry and hydrated particle diameters for PAM using LD reported in d_{V-LD}, d_{SA-LD}, and d_{N-LD} along with d_{OM} are shown in Figure 7A and Figure 7B respectively. Scaling on the y-axis is not the same for both plots due to the large difference in particle diameters between dry and hydrated SAP. It should be noted that the standard deviations (error bars) shown for LD measurements do not represent the error between sample measurements that may be associated with the measurement method but rather the variation between each individual particle measurement and therefore correlates to the width of the PSD.

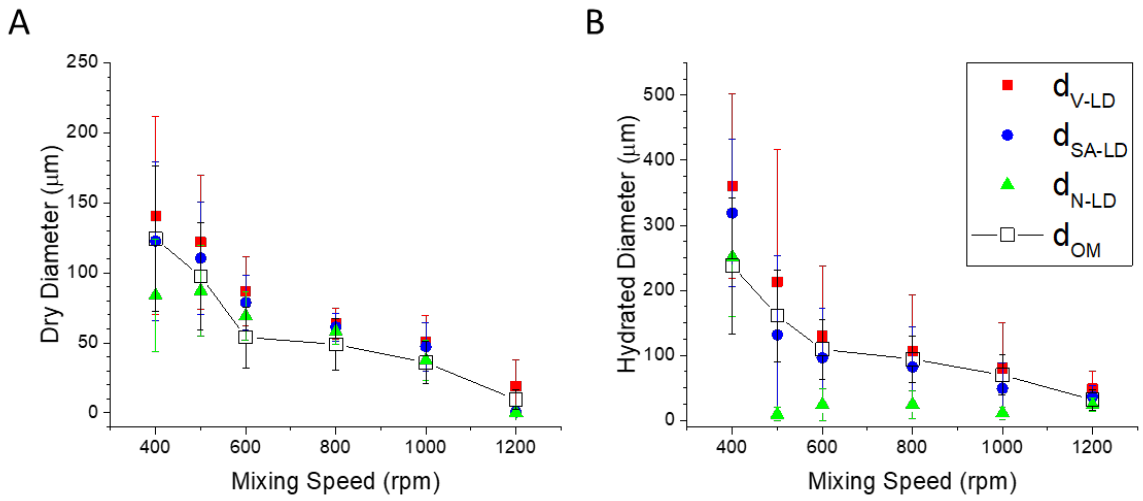

Figure 7: Average dry (A) and hydrated (B) volume **(d_{V-LD})**, surface area **(d_{SA-LD})**, and number **(d_{N-LD})** mean particle diameters and standard deviations for PAM using laser diffraction with optical microscopy number mean particle diameters **(d_{OM})**.

Figure 7A shows that dry particle size measurements using LD (suspended in 2-propanol) are consistent with OM measurements and follow the same trends. When comparing the three LD PSD outputs, it can be seen that d_{V-LD} has the largest average diameter at all mixing speeds while d_{N-LD} has the smallest due to how the particle size calculations are weighted. Figure 7B shows similar average hydrated particle diameters, size distributions and trends between LD and OM: d_{V-LD} is the largest diameter at all mixing speeds; d_{SA-LD} align closest with d_{OM}, never falling outside of one standard deviation; d_{N-LD} show little to no trend with mixing speed and are typically

the lowest average diameters presented. Comparing d_{V-LD} to d_{N-LD} shows that a greater percentage of particles at each mixing speed are small (as seen in Figure 6B) while the majority of swelling and water storage occurs in a relatively low percentage of large particles. This may also indicate that some particles do not swell as much as others, or at all, resulting in the small d_{N-LD} values that are observed. As shown in Figure 6, as the mixing speed increases, all diameter values converge to similar values and standard deviations for each measurement become smaller, confirming that there is a more narrow size distribution at higher mixing speeds. Consistency between OM and LD ensures that the size measurements are accurate and increases the confidence of the determined particle sizes.

3.4 Estimates of Swelling Capacity

Swelling capacity for PAM particles at various mixing speeds using the gravimetric method is shown in Figure 8. Nylon filter bags were used due to their small pore size. When using commercial tea bags, which typically contain larger pore sizes, it was found that SAP was able to diffuse through the larger pores resulting in a reduction in measured swelling capacity and inconsistent data due to the lost mass.

PAM was found to have an equilibrium swelling capacity between 6 and 11 grams of water per gram of dry SAP. Equilibrium swelling occurs within 1 minute for the 600, 800, and 1000 rpm PAM samples and within 3 minutes for the 500 rpm sample. Swelling kinetics are dependent on particle size (i.e., the mixing speed during synthesis) while there is no significant trend between the equilibrium swelling capacity and particle size, consistent with previous work [40]. Since a trend does not exist, the swelling capacity of PAM can be reported as an average of the equilibrium swelling capacity at all mixing speeds. This gives an average swelling capacity of 8.2 ± 0.37 grams of water per gram of SAP.

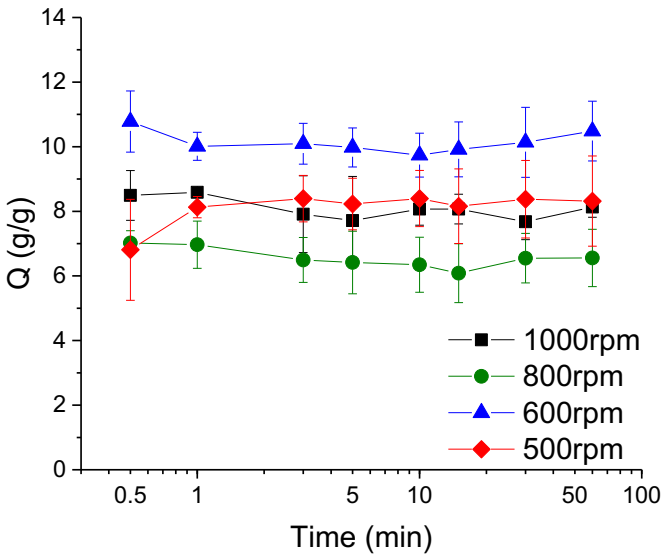

Figure 8: Swelling capacity in nanopure water using the gravimetric method for PAM synthesized at mixing speeds of 1000, 800, 600 and 500 rpm. Error bars represent 95% confidence intervals. Time is plotted on a logarithmic scale.

While there is no correlation between the speed of mixing and the resulting Q value, there is a spread of Q values between samples. This variation could be due to random inconsistencies during the polymerization process. Each batch of SAP is made individually which could introduce some variation in the amount of crosslinker used between samples. These small errors from sample to sample could result in differences between the crosslinking density and ultimately be responsible for the spread of swelling capacities [2]. An increase in crosslinking results in reduced swelling values while less crosslinking yields increased swelling capacities [17,22,31,36].

Using data collected from OM and LD, Table 3 shows the average calculated swelling capacities due to volume change for SAP. Volume mean diameter was used when calculating the volume change of SAP from the dry state to hydrated state. Swelling capacity is best described by volume diameter because these values describe the particles that account for the majority of swelling and water storage. As discussed in section 3.3, number diameter shows small particle sizes at all mixing speeds and may not account for the relatively few particles that are contributing to the majority of water storage.

Table 3: Average swelling capacity and 95% confidence intervals for PAM using the gravimetric method and volumetric method via optical microscopy and laser diffraction.

Method	Gravimetric	Optical Microscopy	Laser Diffraction
Q (g/g)	8.2 ± 0.37	6.5 ± 3.8	5.7 ± 3.9

Table 3 shows that the volumetric method can be used to calculate the swelling capacity of spherical SAP particles. Using this method, swelling capacities are similar to those found when using the gravimetric method but are slightly lower and have larger confidence intervals.

An increase (or over-estimation) in the measured swelling capacity when using the gravimetric method, may be due to the presence of excess water between particles. When using this method, particles are submerged into water and then weighed. During the weighing process the bulk mass is measured, including any excess water that is on the surface of the particles, trapped water between neighboring particles, and any water absorbed by the filter bag. This water contributes to the swelling capacity as though it were water absorbed by the SAP particles, resulting in a slightly larger observed swelling capacity [28]. Swelling measurements using the volumetric method eliminate the contribution of excess water to the calculation of absorbed water. In this method, absorbed water is calculated by measuring a change in volume and does not take into account any excess water that is trapped between particles.

Some particles were observed to contain surface defects in optical micrographs of particles in their dry (unhydrated) state – see arrows in Figure 5 These collapsed regions of the particle's surface most likely resulted from regions of low polymer concentration in the internal polymer network and perhaps a nonuniform concentration of crosslinks. Such low-density regions would be visible as surface defects when the particles are dry and notably absent when the particles are hydrated (as they would fill with water; refer to Figure 5). As some of the dry particles are not perfect spheres but instead contain collapsed regions on their surface, these surface defects may contribute to the differences found in calculated swelling capacities. A perfect sphere is assumed when calculating V_d for OM and LD. This assumption leads to an overestimation of V_d in Equation 2 and ultimately an underestimation in Q_V. While these surface defects may contribute to some underestimation when calculating Q_V , it would not account for the large difference that was found

between methods (Q_V is approximately 36% lower than Q_g) as the surface defects are uncommon and often small in size.

Volumetric swelling measurements using OM and LD resulted in larger confidence intervals due to the large PSD in each sample. Error may also arise when using OM because individual particles were not tracked from the dry to hydrated state but instead many dry and hydrated particles were randomly selected and measured. Gravimetric swelling measurements have relatively narrow confidence intervals because the sample being tested is treated as one macroscale object and not individual particles, eliminating any variation in swelling between particles. To reduce the error associated with the volumetric method, specifically OM, an individual particle swelling study was carried out to increase the confidence and identify/eliminate error in swelling capacity measurements.

Figure 9 shows micrographs of three individual particles in the dry and hydrated state. Using the volumetric method (OM), the swelling capacities of particles 1, 2, and 3 were calculated to be 4.7, 3.3 and 7.0 g/g respectively. Micrographs were taken for 30 different particles and swelling capacities were calculated for each one. A distribution of the 30 individual particle volumetric swelling capacity measurements as well as gravimetric measurements (for a collection of particles from the same batch as the 30 individual particles) can be seen in Figure 10A and Figure 10B respectively. These calculations resulted in an average swelling capacity of 5.2 ± 0.66 g/g and is similar to what was previously found using OM and average particle sizes but has a significant decrease in the confidence interval. Individual particle swelling capacity values are closest to the swelling capacities found using LD, indicating the accuracy of these two methods.

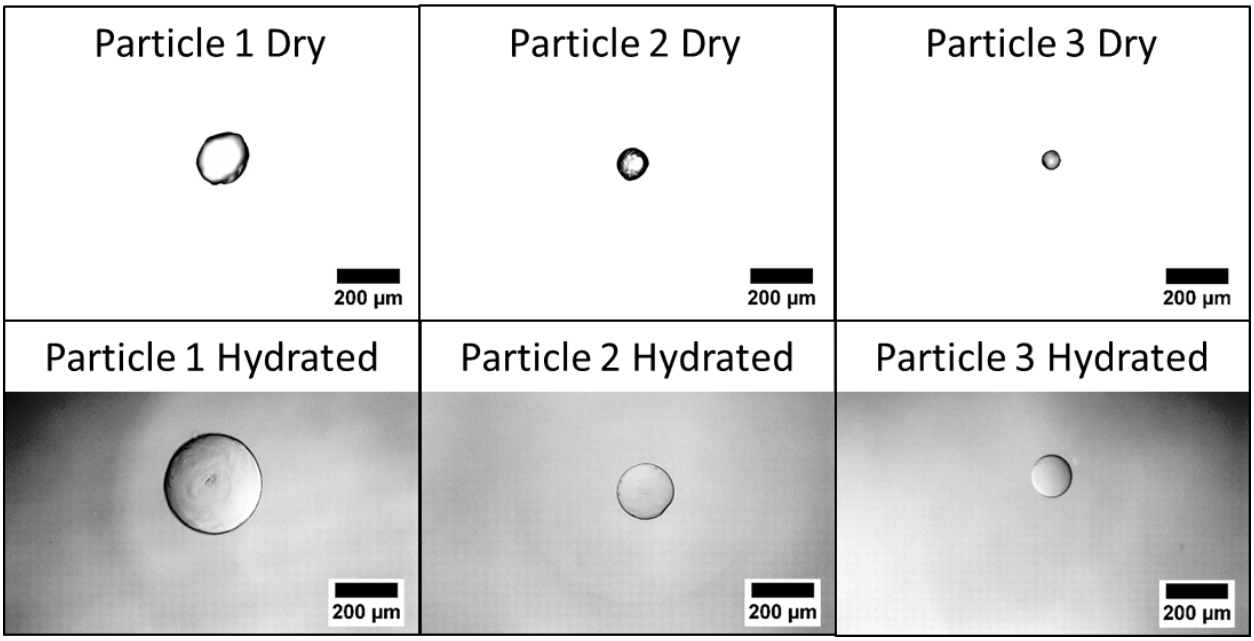

Figure 9: Micrographs of dry and hydrated particles for single particle swelling studies. Scale bars are 200 µm.

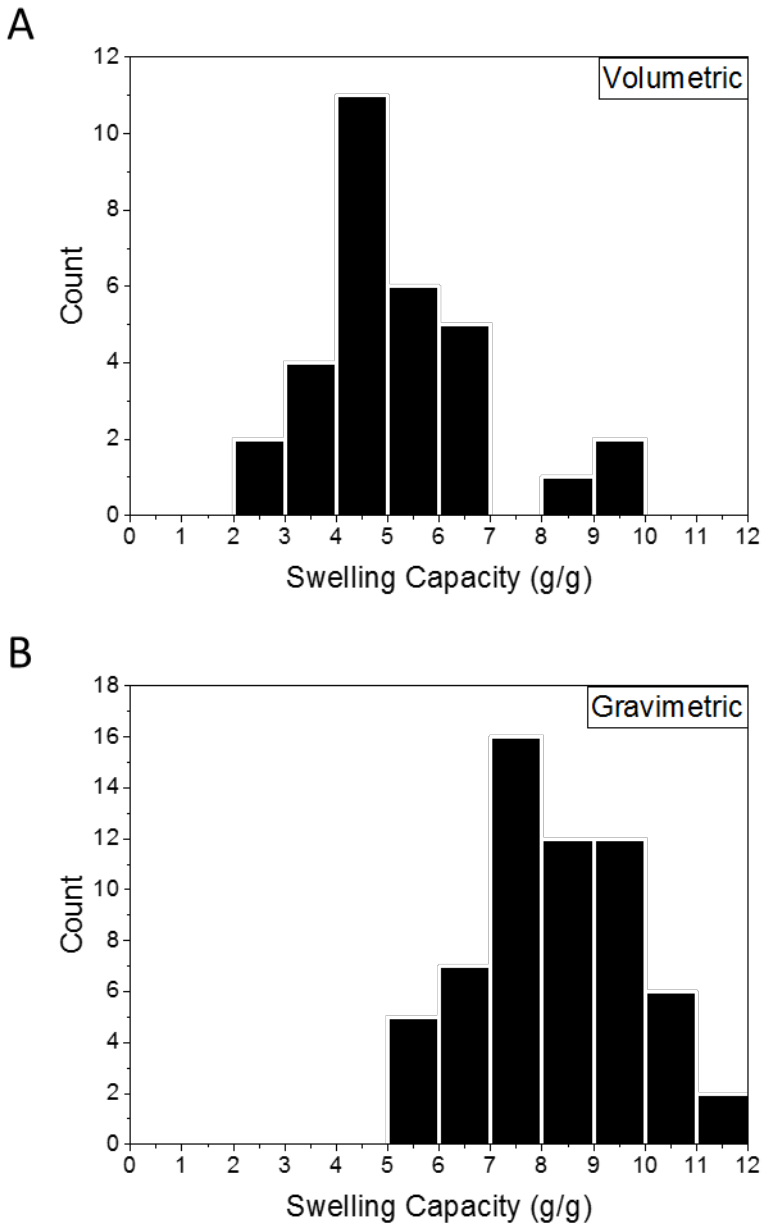

Figure 10: Swelling capacity measurement distributions using the volumetric (A) and gravimetric (B) methods. A total of 30 measurements were made for the volumetric method and 60 measurements were made for the gravimetric method.

Comparing the gravimetric method to the volumetric method (data from Figure 10), it can be concluded with 99.99% confidence (p-value of less than 0.00001) that the calculated swelling capacities are significantly different and that the volumetric method results in a reduced – and most likely more accurate – measure of swelling capacity. With 95% confidence, the volumetric method resulted in swelling capacities that are between 2.2 and 3.7 g/g lower than the gravimetric method.

This suggests that for one gram of dry SAP, about 3 grams of water can be contributed to excess water within the sample used for gravimetric measurements.

4 Summary and Conclusions

Inverse suspension polymerization successfully produced spherical SAP particles. As the mixing speed increased from 400 rpm to 1200 rpm, the average particle diameter and size distribution decreased. In determining the PSDs, OM and LD proved to be consistent with each other, suggesting accurate PSD measurements for SAPs in the dry and hydrated state. Ethanol and 2-propanol were found to be suitable solvents to suspend dry PAM particles when using LD. It was found that LD d_{SA-LD} aligned closest with d_{OM}, while d_{V-LD} resulted in the largest particle sizes, which were much larger than d_{N-LD} in the hydrated state. This large difference between d_{V-LD} and d_{N-LD} suggests that there were relatively few, large particles responsible for the majority of the SAP's swelling capacity. All three PSDs that are obtained through LD (i.e., d_{V-LD}, d_{SA-LD}, and d_{N-LD}) contain valuable information on the particles responsible for the water storage, water transfer, and the number of particles at a specific size, respectively.

Gravimetric swelling measurements resulted in swelling capacities between 6 and 11 g/g and were not dependent on particle size. Equilibrium swelling occurred within 3 minutes of being submerged in nanopure water and was dependent on particle size, as smaller particles achieved equilibrium more quickly. Volumetric swelling capacity measurements were separately calculated using OM paired with ImageJ and from LD volume mean diameters. These measurements resulted in a statistically significant reduction in the calculated swelling capacities when compared to gravimetric calculations, as excess (nonabsorbed) water between neighboring particles was not accounted for in OM and LD. Thus, the swelling capacities determined from the volumetric methods (OM and LD) are believed to be more accurate compared to the gravimetric methods, further evidenced by the similar results from individual particle swelling experiments. In practice, LD has some benefits compared with OM: it can detect large (> 500 μm) and small (< 20 μm) particles that can go unnoticed when using OM, and it is less time consuming to determine PSDs and swelling capacities.

5 Acknowledgements

C.D. acknowledges funding obtained from the Purdue University Summer Undergraduate Research Fellowship Program. Additionally, this material is based upon work supported by the National Science Foundation (Grant Number 1454360) and the donors of The American Chemical Society Petroleum Research Fund (Grant Number 54886-DNI10).

6 References

1. Wei, Q.-B., Luo, Y.-L., Fu, F., Zhang, Y.-Q., Ma, R.-X. *J. Appl. Polym. Sci.*, 2013, **129**, 806–814.

2. Shi, D., Gao, Y., Sun, L., Chen, M. *Polym. Sci. Ser. A*, 2013, **56**, 275–282.

3. Zohuriaan-Mehr, M. J., Kabiri, K. *Iran. Polym. J.*, 2008, **17**, 451–477.

4. Bo, Q., Ling, Y., Jun, L., Wang, Q., Jun, D. *Polym. Sci. Ser. A*, 2011, **53**, 707–714.

5. Hüther, A., Xu, X., Maurer, G. *Fluid Phase Equilib.*, 2004, **219**, 231–244.

6. Mechtcherine, V., Reinhardt, H. W. Application of Super Absorbent Polymers (SAP) in Concrete Construction, RILEM State of the Art Report 2, Dresden , Germany, 2012.

7. Jensen, O. M., Hansen, P. F. *Cem. Concr. Res.*, 2002, **32**, 973–978.

8. Krafcik, M. J., Erk, K. A. *Mater. Struct.*, 2016, **49**, 4765–4778.

9. Rai, U. S., Singh, R. K. *Mater. Sci. Eng. A*, 2005, **392**, 42–50.

10. Sun, Z., Xu, Q. *Mater. Sci. Eng. A*, 2008, **490**, 181–192.

11. Deligkaris, K., Tadele, T. S., Olthuis, W., van den Berg, A. *Sensors Actuators, B Chem.*, 2010, **147**, 765–774.

12. Hoare, T. R., Kohane, D. S. *Polymer (Guildf).*, 2008, **49**, 1993–2007.

13. Sahiner, N., Godbey, W. T., McPherson, G. L., John, V. T. *Colloid Polym. Sci.*, 2006, **284**, 1121–1129.

14. Wang, B., Lin, M., Guo, J., Wang, D., Xu, F., Li, M. *J. Appl. Polym. Sci.*, 2015, **133**, 1–7.

15. Zou, C., Zhao, P., Hu, X., Yan, X., Zhang, Y., Wang, X., Song, R., Luo, P. *Energy and Fuels*, 2013, **27**, 2827–2834.

16. Li, X., Liu, X., Chen, Q., Wang, Y., Feng, Y. *J. Macromol. Sci. Part A*, 2010, **47**, 358–367.

17. Lu, S., Cheng, G., Pang, X. *J. Appl. Polym. Sci.*, 2006, **100**, 684–694.

18. Justs, J., Wyrzykowski, M., Bajare, D., Lura, P. *Cem. Concr. Res.*, 2015, **76**, 82–90.

19. Schrö, C., Mechtcherine, V., Gorges, M. *Cem. Concr. Res.*, 2012, **42**, 865–873.

20. Du, J., El-sherbiny, I. M., Smyth, H. D. *AAPS Pharm SciTech*, 2014, **15**, 1535–1544.

21. Gavini, E., Rassu, G., Muzzarelli, C., Cossu, M., Giunchedi, P. *Eur. J. Pharm. Biopharm.*, 2008, **68**, 245–252.

22. Shimizu, H., Wada, R., Okabe, M. *Polym. J.*, 2009, **41**, 771–777.

23. Eshel, G., Levy, G. J., Mingelgrin, U., Singer, M. J. *Soil Sci. Soc. Am. J.*, 2004, **68**, 736–743.

24. Kurkuri, M. D., Aminabhavi, T. M. *J. Control. Release*, 2004, **96**, 9–20.

25. Pellegrini, M., Cherukupalli, A., Medini, M., Falkowski, R., Olabisi, R. *Tissue Eng. Part C*, 2015, **21**, 1246–50.

26. El-Sherbiny, I. M., Smyth, H. D. C. *Int. J. Pharm.*, 2010, **395**, 132–141.

27. El-Sherbiny, I. M., McGill, S., Smyth, H. D. C. *J. Pharm Sci.*, 2010, **99**, 2343–2356.

28. Esteves, L. P. *Mater. Struct.*, 2015, **48**, 2397–2401.

29. Malvern Instruments A Basic Guide to Particle Characterization, Worcestershire, UK, 2015.

30. Lee, H. *Adv. Appl. Ceram.*, 2010, **109**, 296–302.

31. Tripathi, R., Mishra, B. *AAPS Pharm SciTech*, 2012, **13**, 1091–1102.

32. Haynes, W. H. CRC Handbook of Chemistry and Physics, CRC Press, Boca Raton, 91st edn., 2011.

33. Van Krevelen, D. W., Nijenhuis, K. T. Properties of Polymers - Their Correlation with Chemical Structure; Their Numerical Estimation and Prediction from Additive Group Contributions, Elsevier, 4th edn., 2009.

34. Vivaldo-Lima, E., Wood, P. E., Hamielec, A. E., Penlidis, A. *Ind. Eng. Chem. Res.*, 1997, **36**, 939–965.

35. Odian, G. Principles of Polymerization, John Wiley & Sons, Inc., 3rd edn., 1991.

36. Mah, E., Ghosh, R. *Processes*, 2013, **1**, 238–262.

37. Wu, S., Shanks, R. A. *J. Appl. Chem.*, 2004, **93**, 1493–1499.

38. Wakai, C., Oleinikova, A., Ott, M., 1rtner, H. W. *J. Phys. Chem. B Lett.*, 2005, **109**, 17028–17030.

39. Wypych, G. Handbook of Solvents, ChemTec Publishing, Toronto, 2001.

40. Zhu, Q., Barney, C. W., Erk, K. A. *Mater. Struct.*, 2015, **48**, 2261–2276.